Discrimination of Single Mutations in Cancer-Related Gene Fragments with a Surface Acoustic Wave Sensor

ARTICLE *in* ANALYTICAL CHEMISTRY · AUGUST 2006

Impact Factor: 5.64 · DOI: 10.1021/ac060296c · Source: PubMed

4 AUTHORS, INCLUDING:

Thomas M A Gronewold
Eurofins, Germany
34 PUBLICATIONS **886** CITATIONS

SEE PROFILE

Anal. Chem. **2006,** *78,* 4865−4871

Discrimination of Single Mutations in Cancer-Related Gene Fragments with a Surface Acoustic Wave Sensor

Thomas M. A. Gronewold,† Antje Baumgartner,† Eckhard Quandt,† and Michael Famulok*,‡

LIMES Program Unit Chemical Biology & Medicinal Chemistry, c/o Kekulé Institute for Organic Chemistry and Biochemistry, University of Bonn, Gerhard-Domagk-Strasse 1, 53121 Bonn, Germany, and Research Center CAESAR, Ludwig-Erhard-Allee 2, 53175 Bonn, Germany

Here, we report on using a surface acoustic wave sensor for the highly sensitive and accurate detection of individual point mutations in cancer-related gene DNA fragments from single injections. Our sensor measures both the mass and viscosity signals and, thus, allows discriminating between mass effects resulting from hybridization of short DNA strands and viscosity effects due to increasing amounts of DNA deposited on the sensor. Single nucleotide exchanges or deletions are distinguished reliably and with exceeding simplicity from the wild-type sequences, on the basis of differences in their dissociation or association rates starting at low nanomolar concentrations. Mutant oligonucleotides were identified immediately from viewing the recorded signal and without further processing of the data. Multiple repeated binding cycles were possible over days without affecting sensitivity. To achieve signal amplification, our new bioassay can also apply multiple hybridization steps based on sandwich hybridizations. Kinetic evaluations gave insight into the physicochemical properties of the fragments used that explain the differences in their binding processes.

Among the most challenging and demanding aspects of determining hybridization events is the rapid and reliable detection of single mutations within a nucleic acid. This is useful for discovering single-nucleotide polymorphisms or mutations in disease-related gene fragments for a variety of research and diagnostic applications, including broad-scale genetic testing.[1] The identification of etiological defects in genetic diseases has improved diagnosis and treatment in symptomatic patients and allows prediction of risks of future disease in asymptomatic individuals to prevent some of these diseases by early intervention,[2,3] and successful treatment of most cancers depends on early detection and identification. Mutations associated with cancer can be inherited (germline) or acquired (somatic).[4] In addition, genetic alterations can arise during tumorigenesis.[3] Due to its stability under the fairly harsh conditions clinical samples often have to undergo, DNA appears to be an ideal substrate for molecular diagnosis. Methods based on DNA−DNA hybridization of wild-type and complementary mutant fragments often use fluorescence labeling to achieve sufficient specificity. This is put to use, for example, for pairs of DNA from symptom-free individuals with DNA from patients with symptoms.[5] A variety of label-free sensor systems were developed using acoustic, electronic, and optical detection methods.[6] In combination with DNA hybridization events, biosensors have been created for different applications, for example, repeated measurements of elongation,[7] gravity,[8] the relation between distance to the sensor surface and measured signal and the viscoelastic property of a bound DNA strand,[9,10] and determination of single-point mutations in oligonucleotides.[10,11] However, high sensitivity often requires labeling of the DNA, or differences are enhanced by thermal elevation and stringency washes, or tools, such as nanoparticles or time-consuming gel-based methods, are necessary. Both quartz crystal microbalances (QCM) and surface acoustic wave (SAW) sensors are sensitive to the mass of the unbound species as well as to viscoelastic properties of the surrounding liquid and layers of bound biological material. The ability of our Love-wave SAW sensor to independently extract the pure mass and viscosity signal of a deposited layer[2] is unique. This makes the sensor especially useful for investigating DNA−DNA interactions with high sensitivity. Binding of short DNA strands affects the mass fraction of the sensor

* To whom correspondence should be addressed. E-mail: m.famulok@uni-bonn.de.

‡ University of Bonn.

† Research Center CAESAR.

(1) Strerath, M.; Marx, A. *Angew. Chem., Int. Ed.* **2005**, *44*, 7842−7849.
(2) Ponder, B. *Science* **1997**, *278*, 1050−1054.
(3) Sidransky, D. *Science* **1997**, *278*, 1054−1059.
(4) Demant, P. *Radiat. Res.* **2005**, *164*, 462−466.
(5) (a) Erickson, D.; Liu, X.; Venditti, R.; Li, D.; Krull, U. J. *Anal. Chem.* **2005**, *77*, 4000. (b) Wabuyele, M. B.; Farquar, H.; Stryjewski, W.; Hammer, R. P.; Soper, S. A.; Cheng, Y.-W.; Barany., F. *J. Am. Chem. Soc.* **2003**, *125*, 6937.
(6) (a) Mirkin, C. A.; Letsinger, R. L.; Mucic, R. C.; Storhoff, J. J. *Nature* **1996**, *382*, 607. (b) Niemeyer, C. M. *Angew. Chem., Int. Ed.* **2001**, *40*, 4129. (c) Wang, J.; Xu, D.; Kawde, A. N.; Polsky, R. *Anal. Ch*em**. 2001***, 73*, 5576. (d) Park, S. J.; Taton, T. A.; Mirkin, C. *A. Science* **2002***, 295*, 1503. (e) Bailey, R. C.; Nam, J. M.; Mirkin, C. A.; Hupp, J. *T. J. Am. Chem. Soc.* **2003**, *125*, 13541.
(7) Buckle, M.; Williams, R. M.; Negroni, M.; Buc, H. *Proc. Natl. Acad. Sci. U.S.A.* **1996**, *93*, 889−894.
(8) Fawcett, N. C.; Craven, R. D.; Zhang, P.; Evans, J. A. *Langmuir* **2004**, *20*, 6651−6657.
(9) Glass, S.; Schlensog, M. D.; Gronewold, T. M. A.; Kiwitz, A.; Gorski, R.; Stoyanov, I.; Perpeet, M.; Tewes, M.; Löhndorf, M.; Quandt, E. *Sens. Actuators, B*, in press.
(10) Höök, F.; Ray, A.; Nordén, B.; Kasemo, B. *Langmuir* **2001**, *17*, 8305.
(11) Wittung-Stafshede, P.; Rodahl, M.; Kasemo, B.; Nielsen, P.; Norden, B. *Colloids Surf., A* **2000**, *174*, 269.

10.1021/ac060296c CCC: $33.50
Published on Web 06/15/2006

signal, whereas in prolonged strands, the viscosity fraction becomes predominant until they behave like a purely viscous layer close to the sensor surface.[9,10]

EXPERIMENTAL SECTION

All chemicals were of analytical grade and were used as received. 11-Mercaptoundecanoic acid (45,056-1) was obtained from Aldrich; *N*-(3-dimethylaminopropyl)-*N*′-ethylcarbodiimide hydrochloride (EDC, 8.00907.0005), from Merck; *N*-hydroxysuccinimide (NHS, H-7377) and dextran from *Leuconostoc mesenteroides* (D1037), from Sigma; and streptavidin (S888), from Molecular Probes. Oligonucleotides were commercially synthesized by Operon. Names and sequences of the oligonucleotides used are summarized in Supporting Information Table 1. Buffer solutions for dilutions and running buffers were prepared in distilled, deionized water. All oligonucleotide stocks were stored in ddH_2O at −20 °C.

The Love-wave sensor (S-sens) allows recording the phase shift, φ, and the viscosity, η, at a constant frequency due to binding of molecules to the surface. The sensor consisted of an ST-cut quartz sensor chip containing five sensor elements and a surface acoustic wave reader.[12] Thin gold films are supported on processed silicon wafers. The sulfur headgroups of organosulfur compounds bind as thiolates to gold surfaces and create a self-assembled monolayer (SAM).[13] A carboxymethylated dextran layer was prepared on a SAM of 11-mercaptoundecan-1-ol.[14] Surface preparation was performed in flow-through. The carboxyl groups were activated with 200 mM *N*-ethyl-*N*-(dimethyaminopropyl)-carbodiimide (EDC) and 50 mM *N*-hydroxysuccinimide (NHS) to bind 200 μg/mL streptavidin S888 (Molecular Probes), forming carboxylamides. An excess of activated unreacted NHS esters was deactivated by 1 M ethanolamine, pH 8.5. Biotinylated oligonucleotides (BioTEG) were attached to the sensor chip surface in PBS buffer containing 1 mM $MgCl_2$. This was accomplished through binding of the biotin residues to the immobilized streptavidin. Oligonucleotides were hybridized, and dilutions were performed in DNA binding buffer containing 10 mM Tris−HCl, pH 8.3, 1.5 mM $MgCl_2$, 50 mM KCl, which was also used as running buffer. It was possible to fully regenerate the surface down to the coupled first strand with an injection of ddH_2O. Mobile oligonucleotides were injected at a flow rate of 40 μL/min and an injection volume of 200 μL. The total contact time was ∼300 s.

The system used is based on specific binding of one-half of the oligonucleotides to an oligonucleotide probe. The second half is left unbound and free for specific binding of the next oligonucleotide. In each injection, one single and specifically bound layer is formed. Each mobile strand binds to the previously bound strand by an overlap of 10 bases and links to the next by another 10-base tract. Excess, nonhybridized DNA was expelled from the cell with the running buffer.

The genes investigated are related to some of the most common genetically based cancers. Published sequences from patients were screened, and single fragments with frequent point mutations were selected. The oligonucleotides were assured to be selected so as to avoid dimerization and hairpin formation to exclude random binding events. Sequences are described in Supporting Information Table 1.

BRCA1, the breast cancer susceptibility gene 1, is a tumor suppressor gene. Mutations have caused hereditary breast cancer,[15] but also ovarian, and prostate cancers.[16] The mutation selected is a T → G-exchange (a guanosine for a thymidine). As a second example, sequences were drawn from the human homologue of the *Drosophila melanogaster* patch gene, *ptch*.[17] Mutations in *ptch* cause the most common form of human cancer, nevoid basal cell carcinoma. We selected a deletion of one guanosine nucleotide.[18] The third example is the tumor suppressor gene *p53*, which activates genes that prevent cell growth. Its alteration is associated with ∼50−55% of human cancers. The resulting C → T substitution (a thymidine for a cytosine), as in the mutation selected for the experiments, or CC → TT transitions can lead to skin cancer.[19] It also is commonly altered in tumorigenesis.[3]

RESULTS AND DISCUSSION

The signal of the *BRCA1* sensor depends on the properties of the contacting fluid and consists of the coupling of mass to the sensor surface but also its viscosity. For any interaction with a sensitive layer, the sensor signal directly depends on the distance from the sensor surface. Figure 1B,D shows the overlay plot of the signal of a single experiment. The sensor chip surface was covered with a human *BRCA1* wild-type gene fragment, 5′-biotinTEG-AGGACACTGT-3′. Successively, nonbinding mutated and binding wild-type fragments 5′-AAGGGCCTTCACAGT(→G)-GTCCT-3′ (Supporting Information Table 1) were hybridized (Figure 1A). Consecutive hybridization steps of *BRCA1* complementary fragments carrying a cancer-related point mutation[20] and of wild-type fragments at concentrations from 10 to 5000 nM were monitored. For concise presentation, the change of sensor phase shift signals [%] of selected concentrations of two out of five sensor elements on one sensor array are plotted versus time, each beginning at the start of injection of the mutant strain. The sensor signal for the association of a fragment containing a single mismatch was, on average, 15 ± 4% of that of a fully matched fragment (Figure 1B). In addition, under plain buffer flow, the mismatched fragments dissociated to baseline level within ∼5 min, even at the highest concentrations, whereas matched sequences showed a significantly slower off-rate. The reverse experiments were performed with a sensor chip surface covered with a synthetic oligonucleotide identical to the human *BRCA1* gene fragment carrying the point mutation 5′-biotinTEG-AGGACCCTG T-3′ and successive hybridization of nonbinding wild-type and binding mutated fragments (Figure 1C). Successive hybridization steps of wild-type fragments and of complementary *BRCA1* fragments carrying the point mutation[20] at concentrations from 10 to 5000 nM were monitored (Figure 1D).

(12) Schlensog, M. D.; Gronewold, T. M. A.; Tewes, M.; Famulok, M.; Quandt, E. *Sens. Actuators, B* **2004**, *101*, 308−315.
(13) Schreiber, F. *Prog. Surf. Sci.* **2000**, *65*, 151−256.
(14) (a) Miki, Y.; et al. *Science* **1994**, *266*, 66. (b) Narod, S. A.; Foulkes, W. D. *Nat. Rev. Cancer* **2004**, *2*004, 2665.
(15) Löfås, S.; Johnsson, B. *J. Chem. Soc., Chem. Commun.* **1990**, *21*, 1526.
(16) Turner, N.; Tutt, A.; Ashworth, A. *Nat. Rev. Cancer* **2004**, *4*, 814.
(17) Johnson, R. L.; Rothman, A. L.; Xie, J.; Goodrich, L. V.; Bare, J. W.; Bonifas, J. M.; Quinn, A. G.; Myers, R. M.; Cox, D. R.; Epstein, E. H., Jr.; Scott, M. P. *Science* **1996**, *272*, 1668.
(18) High, A.; Zedan, W. *Curr. Opin. Oncol.* **2005**, *17*, 160.
(19) Brash, D. E.; Rudolph, J. A.; Simon, J. A.; Lin, A.; McKenna, G. J.; Baden, H. P.; Halperin, A. J.; Ponten, J. *Proc. Natl. Acad. Sci. U.S.A.* **1991**, *88*, 10124.
(20) Meindl, A. *Int. J. Cancer* **2002**, *97*, 472.

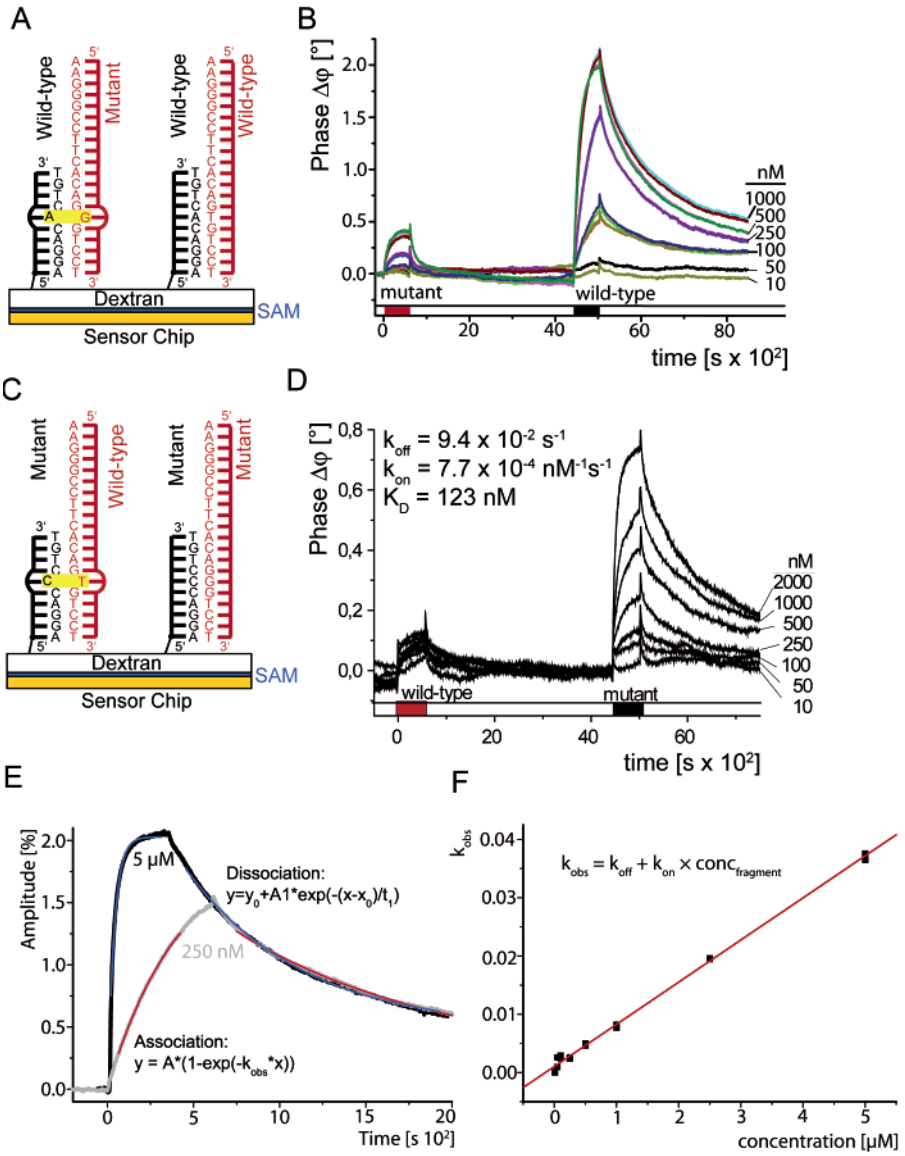

Figure 1. Principle and measurement of DNA oligonucleotide hybridizations. A. Strands carrying the wild-type sequence of a *BRCA1* gene fragment were coupled to a streptavidin-modified dextran layer on the sensor chip via a 5′-biotin linker. B. Combined signals of two sensor elements at different concentrations of analyte DNA. Increasing concentrations of a complementary wild-type (black square) sequence and mutant (red square) *BRCA1* strain were flowed over the surface. Subsequently, buffer was flowed over the surface to dissociate bound fragments (white parts). C. Strands carrying the mutant sequence of a *BRCA1* mutant gene fragment were coupled to a streptavidin-modified dextran layer on the sensor chip via a 5′-biotin linker. D. Combined signals of two sensor elements at different concentrations of analyte DNA. Increasing concentrations of a complementary wild-type (black square) sequence and mutant (red square) *BRCA1* strain were flowed over the surface. Subsequently, buffer was flowed over the surface to dissociate bound fragments (white parts). E. (603 s, gray) and 5000 nM (347 s, black). Fits for association of complementary fragments to surface-bound strands were applied with A = association signal, maximum binding extrapolated to infinite complementary fragment concentration, and k_{obs} = pseudo-first-order kinetic constant. Fits for dissociation of fragments were applied, with y_0 = offset, x_0 = begin buffer injection, A_1 = dissociation signal, and t_1= decay constant (half-life of complex). Fits are shown in red (250 nM) and blue (5 μM). F. k_{obs} values extracted from the sensor signals plotted versus concentration of hybridized fragments. A linear best fit was applied to the data using the equation shown with k_{on} = association rate constant (on-rate) and k_{off} = dissociation rate constant (off-rate).

To determine the association kinetics of the mutant and wild-type fragments to the immobilized detector fragment, respectively, data were extracted from sensor signals for all concentrations using the monomolecular growth model. For determining the corresponding dissociation kinetics, the exponential decay model was assumed. The changes of the sensor phase signals were fitted with Program OriginPro 7G SR3 (OriginLab, Northhampton, MA). Errors for evaluation of association usually were <5% with χ^2-test < 0.0005 and a fraction of variance, R^2 > 0.9. Linear regression had a correlation coefficient of R > 0.998, a standard deviation of <0.001, and a probability measure of <0.0001.

Figure 1E shows the quality of the fits for fully complementary *BRCA1* fragments at two exemplary concentrations, 250 nM and 5000 nM, including the equations used for calculating association and dissociation kinetics. The related kinetic parameters are summarized in Table 1. Surface preparations and binding experiments were performed independently. The curve progression shows that binding at 5000 nM reaches saturation within ~2 min.

Table 1. Kinetic Parameters of *Bcra1* Gene Fragment Association

	$conc_{n_{fragment}}$ (μM)		
	0.25	5	$av_{16plots}$
A (%)	$2 \pm 0.01\%$	$2 \pm 0.002\%$	
k_{obs} (s^{-1})	$2.4 \times 10^{-3} \pm 1 \times 10^{-5}$	$3.8 \times 10^{-2} \pm 3 \times 10^{-4}$	
x_0 (s)	640	362	
y_0 (s)	$0.24 \pm 9 \times 10^{-4}$	$0.26 \pm 7 \times 10^{-3}$	
A_1 (s)	$1.1 \pm 8 \times 10^{-4}$	$1.4 \pm 2 \times 10^{-3}$	
k_{off} (s^{-1})[a] $= 1/t_1$ (s)	$8.47 \times 10^{-4} \pm 8.6 \times 10^{-6}$	$8.44 \times 10^{-4} \pm 1.2 \times 10^{-5}$	$1 \times 10^{-3} \pm 2 \times 10^{-4}$
k_{on} ($nM^{-1}\ s^{-1}$)[a]	6.25×10^{-6}	7.35×10^{-6}	$7.23 \times 10^{-6} \pm 1 \times 10^{-7}$
K_D (nM)[b]	135.5	114.8	143.8

[a] k_{off} and k_{on} were determined from the intercept with the y axis, and from the slope, respectively. [b] K_D was calculated with $K_D = k_{off}/k_{on}$. As a first approximation, $k_{off} = 1/t_1$ and $k_{on} = (k_{obs}\text{-}k_{off})/c$ were extracted from the single plots.

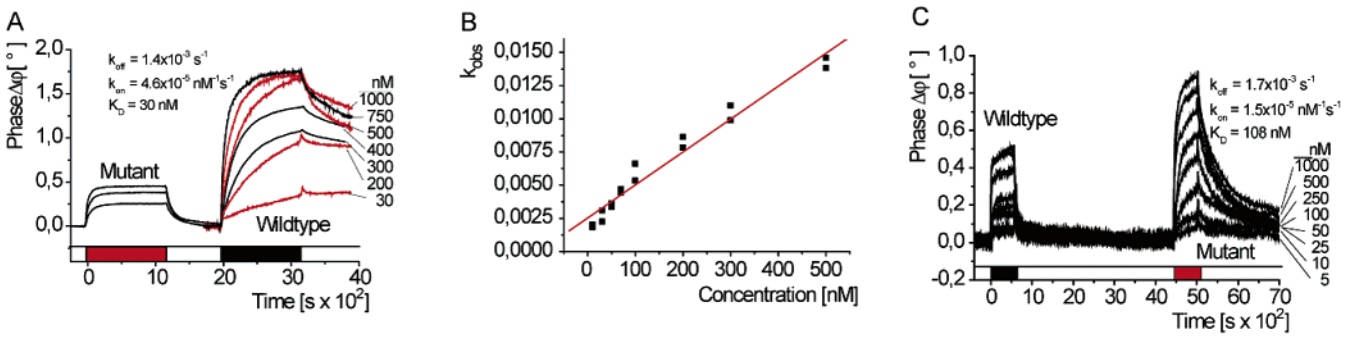

Figure 2. Measurement of *ptch* DNA oligonucleotide hybridizations. A. Signals of two independent measurements with one sensor element at different concentrations of analyte DNA. Prior to the measurements shown, strands carrying the wild-type sequence of a *ptch* gene fragment were coupled to a streptavidin-modified dextran layer on the sensor chip via a 5′-biotin linker. Increasing concentrations of a complementary mutant (red square) sequence and wild-type (black square) *ptch* strain were flowed over the surface. Subsequently, buffer was flowed over the surface to dissociate bound fragments (white parts). B. The k_{obs} values extracted from the sensor signals plotted versus concentration of hybridized fragments. A linear best fit was applied to the data using the equation shown with k_{on} = association rate constant (on-rate) and k_{off} = dissociation rate constant (off-rate). C. Signals of one measurement with one sensor element at different concentrations of analyte DNA. Prior to the measurements shown, strands carrying the mutant sequence of a *ptch* gene fragment were coupled to a streptavidin-modified dextran layer on the sensor chip via a 5′-biotin linker. Increasing concentrations of a complementary wild-type (black square) sequence and mutant (red square) *ptch* strain were flowed over the surface. Subsequently, buffer was flowed over the surface to dissociate bound fragments (white parts).

The association amplitude values (A) differ by only 2%, and the course of dissociation progression is identical for both concentrations, demonstrating excellent reproducibility of independent measurements.

Corresponding fits were applied to the signals shown in Figure 1B, and for each curve, the calculated observed rate constant (k_{obs}) in the association phase was plotted versus concentration to extract the K_D from the resulting straight line using linear regression. The obtained values were $k_{on} = 7.2 \times 10^{-6} \pm 1 \times 10^{-7}$ $nM^{-1}\ s^{-1}$ and $k_{off} = 1 \times 10^{-3} \pm 2 \times 10^{-4}$ s^{-1}, resulting in a $K_D = 144$ nM (Figure 1F). The K_D values extracted from the single plots vary from the average K_D by 6% for the medium fragment concentration of 250 nM and by 20% for the saturation concentration of 5 μM. Thus, for medium concentrations, we can deduce the average K_D value from the sensor signal. For the mutated fragments, the K_D value is more than 20 times higher. For lower concentrations, a K_D cannot be determined accurately.

For the reverse experiment using a surface that carries the mutated *BRCA1* fragment, corresponding fits were applied for binding of *BRCA1* wild-type and fully complementary *BRCA1* mutant fragments. Conversely, the binding affinity of the mutant fragment far exceeds the observed binding of the wild-type fragment. Results for the mutant fragment were $k_{on} = 7.7 \times 10^{-4} \pm 1 \times 10^{-4}$ $nM^{-1}\ s^{-1}$, $k_{off} = 9.4 \times 10^{-2} \pm 6 \times 10^{-3}$ s^{-1}, and a $K_D = 123$ nM.

Similar experiments were performed for other cancer-associated point mutations. For *ptch,* we used the sequences 5′-biotin-TEG-CTCCCCGGTC-3′ and 5′-TTGAGGACAGGACCG(Δ-1)GGGAG-3′. Successive hybridization of nonbinding wild-type and binding mutated fragments at concentrations from 10 to 1000 nM were monitored (Figure 2A), and calculated k_{obs} values were plotted versus concentration of the injected fragments (Figure 2B) to extract kinetic data. Similar to the *BRCA1* mutant fragment, the *ptch* deletion mutant fragment dissociated quickly from the detector strand, whereas the wild-type strain showed an estimated $k_{off} = 1.4 \times 10^{-3} \pm 2.5 \times 10^{-4}$ s^{-1}, $k_{on} = 4.6 \times 10^{-5} \pm 4 \times 10^{-6}$ $nM^{-1}s^{-1}$, and $K_D = 30$ nM (Figure 2C). The parameters for the surface modified with the *ptch*-mutant fragment were $k_{off} = 1.7 \times 10^{-3} \pm 5.5 \times 10^{-5}$ s^{-1}, $k_{on} = 1.5 \times 10^{-5} \pm 4.9 \times 10^{-7}$ $nM^{-1}\ s^{-1}$, and $K_D = 108$ nM.

To apply the sensor for detecting the cancer-related single mutation in *p53*, we used the oligonucleotide 5′-biotin-TEG-CCCAGGACAG-3′ as the detector and the wild-type and mutant sequences 5′-GTGTTTGTGCCTGTC(→T)CTGGG-3′ as the analyte. For this mutant fragment, we found a similar association curve and the same maximums in the phase shift signal as for the wild-type fragment at concentrations from 5 to 2000 nM (Figure 3A). However, the two curves again differed significantly in their dissociation rates. Baseline level is reached for the mutant fragment after $\sim 2 \times 10^3$ seconds. The calculated k_{obs} values were

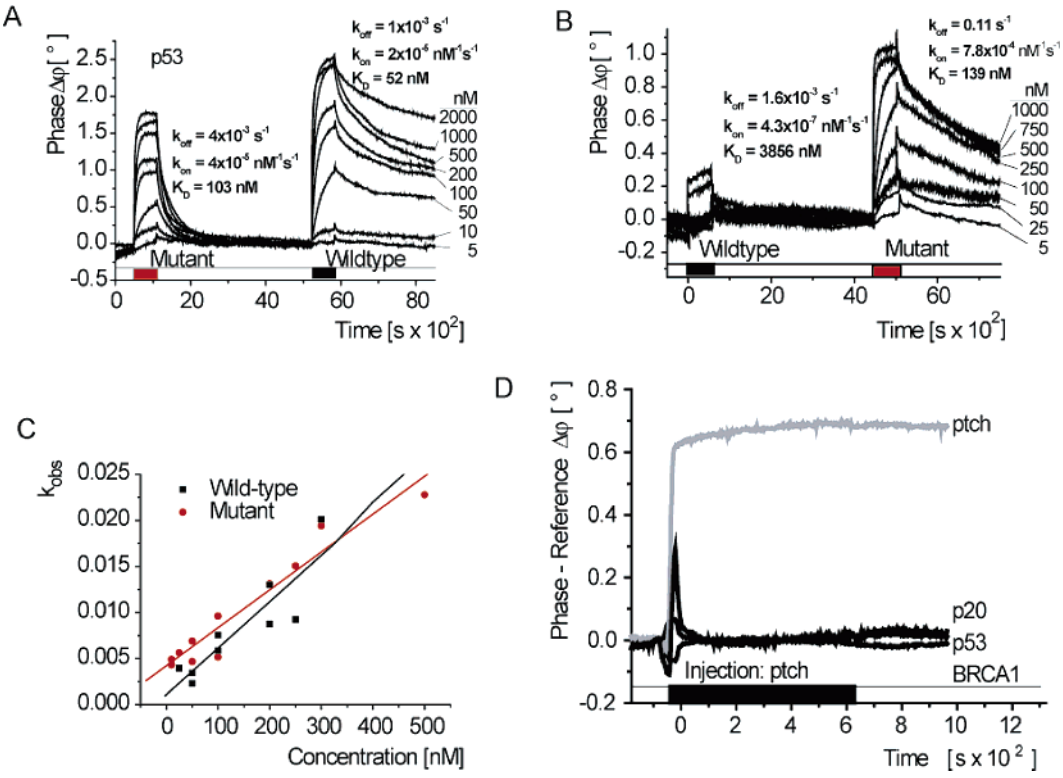

Figure 3. Measurement of *p53* DNA oligonucleotide hybridizations. A. Signals of one sensor element at different concentrations of analyte DNA. Prior to the measurements shown, strands carrying the wild-type sequence of a *p53* gene fragment were coupled to a streptavidin-modified dextran layer on the sensor chip via a 5′-biotin linker. Increasing concentrations of a complementary wild-type (black square) sequence and mutant (red square) *p53* strain were flowed over the surface. Subsequently, buffer was flowed over the surface to dissociate bound fragments (white parts). B. Signals of one sensor element at different concentrations of analyte DNA. Prior to the measurements shown, strands carrying the mutant sequence of a *p53* gene fragment were coupled to a streptavidin-modified dextran layer on the sensor chip via a 5′-biotin linker. Increasing concentrations of a complementary wild-type (black square) sequence and mutant (red square) *p53* strain were flowed over the surface. Subsequently, buffer was flowed over the surface to dissociate bound fragments (white parts). C. The k_{obs} values extracted from the sensor signals plotted versus concentration of hybridized fragments. A linear best fit was applied to the data using the equation shown with k_{on} = association rate constant (on-rate) and k_{off} = dissociation rate constant (off-rate). D. Difference signal of 250 nM *ptch* fragment binding to sensor elements derivatized with the wild-type sequences of gene fragments *ptch* (grey curve), *BRCA1*, *p53*, and oligonucleotide p20 with the sequence 5′-NH_2−$(CH_2)_3$−CTGCATGAGCTAACTACCTG-3′ (black curves). Curves were corrected by the response obtained with a nonderivatized reference element.

plotted versus the concentration of the injected fragment (Figure 3B), which resulted for the wild-type fragment in $k_{off} = 1 \times 10^{-3} \pm 2 \times 10^{-4}$ s^{-1}, $k_{on} = 2 \times 10^{-5} \pm 9.6 \times 10^{-6}$ nM^{-1}s^{-1}, and K_D = 52 nM. The related kinetic parameters for the mutant sequence were $k_{off} = 4 \times 10^{-3} \pm 7 \times 10^{-4}$ s^{-1}, $k_{on} = 4 \times 10^{-5} \pm 3 \times 10^{-6}$ nM^{-1} s^{-1}, and K_D = 103 nM. The similar k_{on} values are based on the strong binding of the detector oligonucleotide. Thus, on the basis of the signal-to-noise ratio after an ~30 min buffer wash, a clear and unambiguous discrimination between the point mutant and the wild-type sequence can be achieved, even though the k_{on} values are similar. The reverse experiments were performed with a sensor chip surface covered with a human *p53* mutant gene fragment carrying the point mutation 5′-biotinTEG-CCCAGAA-CAG-3′. Successive hybridization of nonbinding wild-type and binding mutated fragments at concentrations from 10 to 5000 nM were monitored (Figure 3C). The wild-type fragment has an estimated $k_{off} = 1.6 \times 10^{-3}$ s^{-1}, $k_{on} = 4.3 \times 10^{-7}$ nM^{-1} s^{-1}, and a calculated K_D = 3856 nM. The corresponding mutant fragment resulted in $k_{off} = 0.108$ s^{-1}, $k_{on} = 7.8 \times 10^{-4}$ nM^{-1} s^{-1}, and K_D = 139 nM.

To show that the detection of the cognate DNA occurs specifically, we modified the sensor elements with different cancer fragments. Four out of five sensor elements were derivatized with oligonucleotides corresponding to the wild-type *ptch*, *p20*, and *p53* gene fragments, including a fourth oligonucleotide with no relationship to cancer genes. A fifth sensor element remained underivatized and was used as a reference. Figure 3D shows that the fragment that is complementary to wild-type *ptch* specifically binds only to the element containing the *ptch* strand, but not to the other, noncomplementary base strands, indicating that the sensor detects the cognate sequences highly specifically without any detectable signals for nonmatching DNAs.

We next investigated whether an enhancement of the signal-to-noise ratio can be achieved by sandwich hybridization. As shown in Figure 4, a second DNA fragment was bound to the first mobile strand in an alternating fashion. This leads to an amplification of the signal. Figure 4A,C shows the pure phase and viscosity signals. In Figure 4B,D, the pure mass and viscosity signals were extracted. These data show that the significance of the viscosity signal is much higher than the mass signal for the prolonging DNA strands and that differences are due mainly to the viscoelastic properties of the annealed DNA strands.

The resulting K_D values for the six different base strands were related to the calculated melting temperature T_m. The T_m values

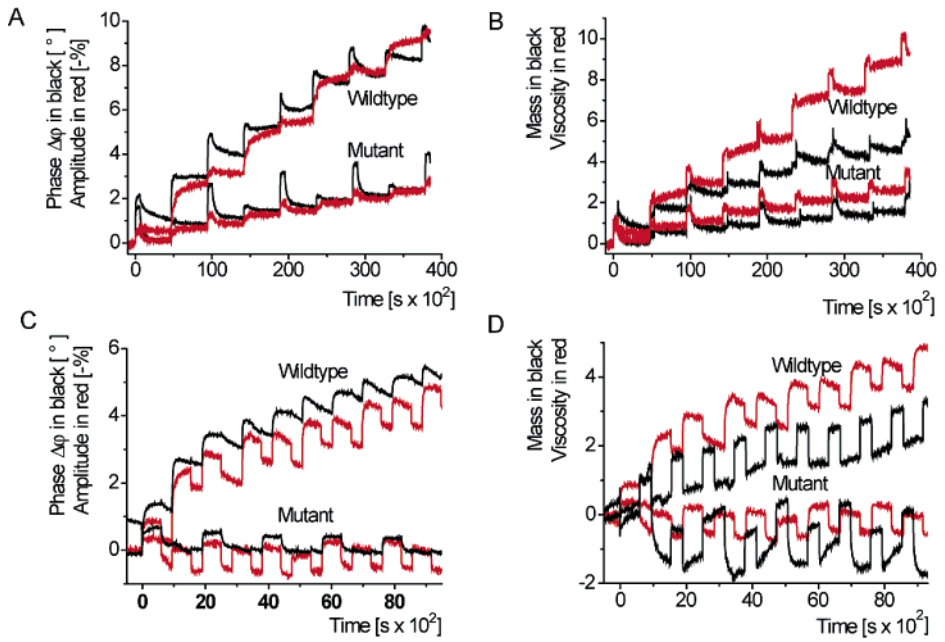

Figure 4. Sandwich hybridization experiment using *p53* and *ptch* fragments. Strands carrying the wild-type sequence of a *p53* gene fragment were coupled to a streptavidin-modified dextran layer on the sensor chip via a 5′-biotin linker. Sensor responses from repeated alternating injections of 1000 nM complementary wild-type fragments and reverse complementary fragments for wild-type and complementary mutant fragments and reverse complementary fragments. A. Phase signal of *p53* in black and amplitude signal in red vs time. B. Extracted mass signal in black of *p53* and extracted viscosity signal in red vs time. C. Phase signal in black of *ptch* and amplitude signal in red vs time. D. Extracted mass signal of *ptch* in black and extracted viscosity signal in red vs time.

for oligonucleotides ranging in length from 20 to 100 residues, and Na^+ concentrations ranging from 0.01 to 1.0 M were calculated using eq 1.

$$T_m = 81.5 + 16.6 \log [Na^+] + 41(G + C)/\text{length} - 500/\text{length} \quad (1)$$

The plot of K_D value versus T_m value (Supporting Information Figure 1) shows the linear correlation of the two values and is, thus, also correlated with the binding and regenerating process of the DNA surface. At very high T_m and very low K_D values, DNA strands differing in a single nucleotide can be differentiated only by the dissociation (Supporting Information Table 2). At lower T_m and higher K_D values, differentiation is already possible on the basis of differences in the association.

CONCLUSIONS

A simple system based on ssDNA sandwich hybridization events with overlapping and unbound parts in each oligonucleotide was shown to discriminate gene fragments differing in one single nucleotide. The results obtained with the *p53* mutant fragments show that cancer-associated single nucleotide exchanges or deletions can reliably be discriminated from the wild-type sequences on the basis of the differences in their dissociation rates that our SAW sensor can readily quantify. The differences in binding behavior are largely influenced by the GC content and the T_m value. Single-base differences in heterozygous DNA result in temperature shifts of 1−5 °C for the lowest melting temperature domain of heteroduplexes, as compared to the fully complementary DNA.[20] But in most cases, the association rates already differ by more than one magnitude. When compared to the fully matching strand, the differing strand is significantly distinguishable in k_{off} value and, for K_D values above 50 nM, from both the differences in association and dissociation rates. The same was proven for the reverse case when the mutant strains were bound to the surface, including *p53* mutant fragment probes. Wild-type fragments showed the same significant differences in association and dissociation and the resulting K_D values as the mutant fragments.

The advantage of using a wild-type sequence as a probe is the possibility to discern several different mutations occurring in the gene fragments hybridized, since the genes subject to testing often contain different mutations in the same region for different tested individuals. On the other hand, testing of specified mutations is possible if mutated probe sequences are used. This is especially important in light of single nucleotide polymorphisms' being the most abundant form of genetic variation. They occur about once every 100−300 bases,[21] and only few or none of them in any subject are related to a pathogenic disease.

Höök et al.[10] used a Q-sens sensor at 15 MHz, allowing combined QCM-D and frequency measurements of oligonucleotides with single mismatches that hybridized to PNA instead of DNA to enhance the signal. They were able to discriminate between mismatch and fully complementary DNA both through kinetics, by comparing reversible and irreversible binding, and total binding at saturation, with a difference below 2-fold, using

(21) Sachidanandam, R.; Weissman, D.; Schmidt, S. C.; Kakol, J. M.; Stein, L. D.; Marth, G.; Sherry, S.; Mullikin, J. C.; Mortimore, B. J.; Willey, D. L.; Hunt, S. E.; Cole, C. G.; Coggill, P. C.; Rice, C. M.; Ning, Z.; Rogers, J.; Bentley, D. R.; Kwok, P. Y.; Mardis, E. R.; Yeh, R. T.; Schultz, B.; Cook, L.; Davenport, R.; Dante, M.; Fulton, L.; Hillier, L.; Waterston, R. H.; McPherson, J. D.; Gilman, B.; Schaffner, S.; Van Etten, W. J.; Reich, D.; Higgins, J.; Daly, M. J.; Blumenstiel, B.; Baldwin, J.; Stange-Thomann, N.; Zody, M. C.; Linton, L.; Lander, E. S.; Altshuler, D. *Nature* **2001**, *409*, 928−933.

measurements giving information about both the mass and viscosity signal. In comparison, the signal-to-noise ratio in our sensor system is considerably better so that we are able to discriminate between mutant and wild-type fragments at every concentration injected, resulting in highly accurate measurements independent of the amounts of injected DNA. This might be due to the typically higher mass sensitivity of SAW sensors at about 148 MHz (sensitivity proportional to frequency squared), the possibility to extract pure mass and viscosity signals, and the small buffer and viscoelastic effects on the measurement due to the two-frequency measurement. Typically, the fully matched sequence showed a 7-fold higher signal than the differing strand. Notably, a single injection is sufficient for determining the K_D value within 2−6% accuracy if the injected concentration is within the range of the K_D value. Far higher or lower concentrations still give a good approximate K_D value.

Without additional thermal elevation or stringency washes and also without the use of time-consuming gel-based methods or enhancing tools as are nanoparticles,[7] single nucleotide exchanges or deletions are differentiated reliably and with exceeding simplicity from the wild-type sequences on the basis of differences in their dissociation or association rates. Multiple repeated binding cycles were possible over days without any difference in sensitivity. The sensor surface was simply regenerated to baseline level by a pulse of ddH_2O. Furthermore, the sensor elements are currently miniaturized to allow parallel measurement of a variety of mutations.

In addition to its high accuracy, reliability, sensitivity, and independence of analyte concentrations, two additional qualities of our approach are notable with respect to potential clinical use. First, fragments complementary to a mutant strain coupled to the surface were shown to give a positive signal for a particular cancer-related mutation fragment but not for the wild-type fragment. This is even more evident for the long DNA strands generated via sandwich hybridization. Since we can use at least five sensor elements, one sensor element could be used as a positive, and one as a negative control, which should further enhance reliability. Second, the surface can easily be regenerated so that a multitude of consecutive measurements are possible. Thus, the method can easily be automated for molecular diagnostic services. Third, we have shown that our SAW-based detection system can reliably discriminate between mass and viscosity effects, a feature that is not possible with other detection systems, such as surface plasmon resonance but that is important for reducing the effect of parameters that cannot easily be controlled (e.g., salt effects, buffer exchanges, or different components in biological samples). Because the SAW-based detection system does not require labeling of the analyte, we believe that this method can easily be adapted to other bioaffinity assays relevant to clinical use.

ACKNOWLEDGMENT

We thank S. Glass, M. Tewes, U. Schlecht, and M. Perpeet for helpful discussions. We also acknowledge A. Kiwitz for the software development of the computer interface, A. Malavé and M. Schlensog for the sensor chip development, and I. Stoyanov for the development of the fluidic system.

SUPPORTING INFORMATION AVAILABLE

Details on oligonucleotide sequences, plot of evaluated K_D values versus melting temperature, and K_D values and properties of the investigated DNA linkers. This material is available free of charge in the Internet at http://pubs.acs.org.

Received for review February 17, 2006. Accepted May 12, 2006.

AC060296C